Refinement and fracture mechanisms of as-cast QT700-6 alloy by alloying method

Min-qiang Gao, *Ying-dong Qu, Rong-de Li, Ke Jiang, and Jun-hua You

School of Materials Science and Engineering, Shenyang University of Technology, Shenyang 110870, China

Abstract: The as-cast QT700-6 alloy was synthesized with addition of a certain amount of copper, nickel, niobium and stannum elements by alloying method in a medium frequency induction furnace, aiming at improving its strength and toughness. Microstructures of the as-cast QT700-6 alloy were observed using a scanning-electron microscope (SEM) and the mechanical properties were investigated using a universal tensile test machine. Results indicate that the ratio of pearlite/ferrite is about 9:1 and the graphite size is less than 40 μm in diameter in the as-cast QT700-6 alloy. The predominant refinement mechanism is attributed to the formation of niobium carbides, which increases the heterogeneous nucleus and hinders the growth of graphite. Meanwhile, niobium carbides also exist around the grain boundaries, which improve the strength of the ductile iron. The tensile strength and elongation of the as-cast QT700-6 alloy reach over 700 MPa and 6%, respectively, when the addition amount of niobium is 0.8%. The addition of copper and nickel elements contributed to the decrease of eutectoid transformation temperature, resulting in the decrease of pearlite lamellar spacing (about 248 nm), which is also beneficial to enhancing the tensile strength. The main fracture mechanism is cleavage fracture with the appearance of a small amount of dimples.

Key words: as-cast QT700-6 alloy; microstructure; graphite; refinement; pearlite lamellar spacing

CLC numbers: TG143.5   **Document code:** A   **Article ID:** 1672-6421(2017)01-016-06

Ductile cast iron has been widely applied in automobile gears and cylinders due to its many desirable properties including high strength, outstanding resistance to wear and oxidation, and high flowability [1]. Nevertheless, the common as-cast ductile iron (QT400-18 or QT700-2) cannot simultaneously achieve high strength and toughness in industrial fields [2-3], mainly because a high strength usually corresponded to a low toughness [4-5]. In the past few years, researchers have been exploring heat treatment methods to improve mechanical properties of ductile cast iron [6-7]. Gonzaga et al. [8] investigated the effect of heat treatment on the ratio of pearlite/ferrite, and it was found that the tensile strength and elongation of ductile iron increased to 687 MPa and 11%, respectively, after normalizing heat treatment at 850 ºC for 1 h, and subsequently cooling in air. Putatunda et al. [9-10] examined microstructures and properties of austempering ductile iron (ADI), and results showed that their performance could be comparable to

that of carbon steels. Although ADI can simultaneously achieve the requirement of high strength and high toughness, the heat treatment process is tremendously complex and will increase production costs [10].

Intensive studies have shown that the alloying method is an effective means to improve the mechanical properties of ductile cast iron by adding aluminum, copper, nickel, stannum chromium and molybdenum, etc. [11, 12]. However, the as-cast ductile cast iron with 700 MPa tensile strength and 6% elongation is difficult to be obtained by alloying method, or even if it can be acquired, its stability is poor [5,12]. Therefore, selecting appropriate elements to prepare the as-cast QT700-6 alloy by alloying method is necessary. Generally, copper and nickel elements have an important role in decreasing the pearlite lamellar spacing [12]. Niobium atoms can react with carbon atoms to form carbide particles as nucleus of heterogeneous nucleation to increase the nucleation rate [13]. Stannum atoms located around the eutectic and graphite can hinder the diffusion of atoms, resulting in grain refinement due to the destruction of grain growth conditions in solidification process [14]. Hence, in this work, the as-cast QT700-6 alloy is synthesized with addition of a certain amount of copper, nickel, niobium and stannum elements. Microstructures, refinement mechanism, pearlite lamellar spacing and

*Ying-dong Qu

Male, born in 1975, Professor, Ph.D. supervisor. His research interests mainly focus on cast alloys.

E-mail: quyingdong@163.com

tensile fracture behavior of the as-cast QT700-6 alloy were investigated.

1 Experimental procedure

Pig iron and scrap steel were first added as raw materials, and then Fe-65%Nb alloy was added to a medium frequency induction furnace. Bulk nickel and copper of 99.99% purity were subsequently added after the furnace charge melting. The stannum bulk was added to the ladle after spheroidizing and inoculation. The 6wt.% Mg-Fe-Si and 75wt.% Si-Fe alloys were used as spheroidizing agent and nucleating agent, respectively. The pouring temperature was 1,450 ºC. Dimensions of the Y type block specimen are shown in Fig. 1. The tensile specimen (Fig. 2) and metallographic specimen (10 mm × 10 mm × 10 mm) were cut from the bottom of the Y type block specimen. Metallographic specimens were etched with 4% nitric acid alcohol for microstructural observation.

Microstructures were observed using scanning-electron microscopes (SEM, Hitachi S-3400N and Hitachi TM3030) equipped with energy-dispersive spectrometers (EDS). Table 1
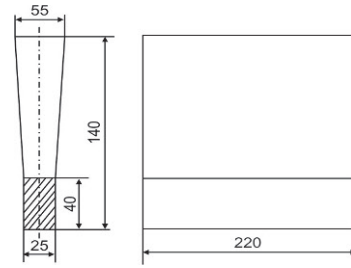

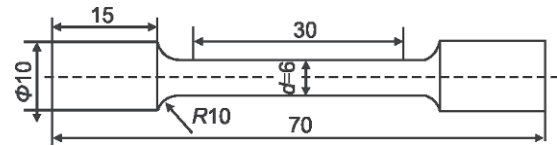**Fig. 1: Dimensions of the Y type block specimen (mm)**

Fig. 2: Dimensions of tensile specimen (mm)

lists the main chemical compositions of as-cast QT700-6 alloy. Carbon equivalent was measured using a CSA-2000 analyzer and tensile testing was performed using a universal tensile machine (WGW-100H) according to GB-T-2002 with a tensile speed of 1.5 mm•min[-1].

Table 1: Chemical compositions of as-cast QT700-6 alloy (wt.%)

| C	Si	Mn	S	P	Cu	Ni	Sn	Nb	Fe
3.50	2.24	0.06	0.023	0.031	0.45	0.86	0.01	0.75	Balance

2 Results and discussion

2.1 Refinement of graphite and niobium carbides in as-cast QT700-6 alloy

Figure 3 shows the microstructure of as-cast QT700-6 alloy. According to GB9441-1988, the grade of spheroidization and graphite size is level 2 and 6, respectively, as shown in Fig. 3(a). Figure 3(b) shows the typical bull's eye microstructure, i.e. the ferrite is encircled around the graphite ball and outer layer is pearlite. Ductile cast iron matrix is usually a mixture of ferrite and pearlite in the as-cast condition [15, 16]. The content of pearlite and ferrite was measured using the image processing method in the LIM-2000 image analysis software, and the ratio of pearlite/ferrite was about 9:1 in the as-cast QT700-6 alloy. Moreover, graphite distribution is relatively homogeneous in different viewing fields in the as-cast QT700-6 alloy. It is well known that the smaller the graphite, the better the mechanical properties of ductile cast iron in a certain range. Therefore, the size and distribution of graphite play an important role in improving mechanical properties of ductile cast iron [17-19]. Generally, graphite with a diameter greater than 50 μm emerges in liquid areas in traditional ductile cast iron according to the Fe-C phase diagram [12]. However, graphite with a diameter less than 40 μm was formed due to the refinement with the addition of niobium element (Fig. 3a).

The affinity between niobium and carbon is relatively strong, leading to the formation of NbC. The reaction between niobium and carbon in the medium frequency induction furnace may take place as follows [20]:

$$[Nb] + [C] = NbC(S) \tag{1}$$
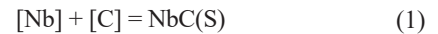
For non-equilibrium solidification, the Gibbs free energy (ΔG_{NbC}) can be expressed as [21]:

$$\Delta G_{NbC} = \Delta G_{NbC}^{\theta} + RTln\frac{1}{\alpha_{[C]} \times \alpha_{[Nb]}}$$
$$= \Delta G_{NbC}^{\theta} - RT\left[lnf_C + lnf_{Nb} + ln[(\%C)(\%Nb)]\right] \tag{2}$$

where ΔG_{NbC}^{θ} is standard equilibrium Gibbs free energy, f_{Nb} and f_C are the activity coefficient of niobium and carbon, respectively. According to equation (2), the formation temperature T of NbC can be obtained when $\Delta G_{NbC}=0$, if the niobium content is a definite value. Then, T is ~1, 180 °C, which is above the eutectoid transformation temperature. It can be proved that niobium carbides were formed in the liquid state.

Figure 4 shows the energy spectrum of the graphite core in as-cast QT700-6 alloy. In general, sulfides and oxides can act as nucleus to promote nucleation [8, 12]. Niobium, sulfur, oxygen and titanium elements are discovered in the graphite core. The niobium carbides formed in the liquid can also act as the heterogeneous nucleus, leading to the increase of nucleation rate and refinement of graphite. Moreover, niobium hinders the carbon from moving during the solidification which also restricts the growth of graphite, and it can also reduce the average diameters of eutectic cells in a certain range [13].

For purposes of comparison, ductile iron with 0.6% niobium
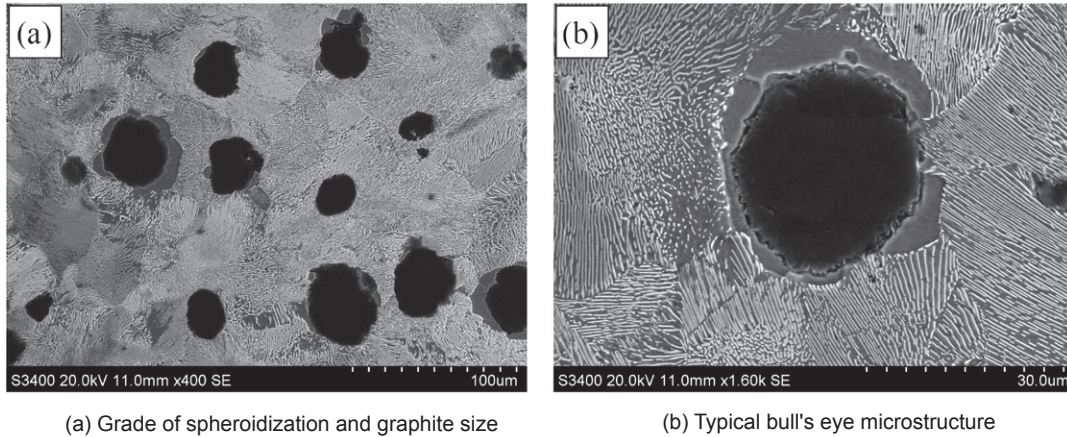
(a) Grade of spheroidization and graphite size

(b) Typical bull's eye microstructure
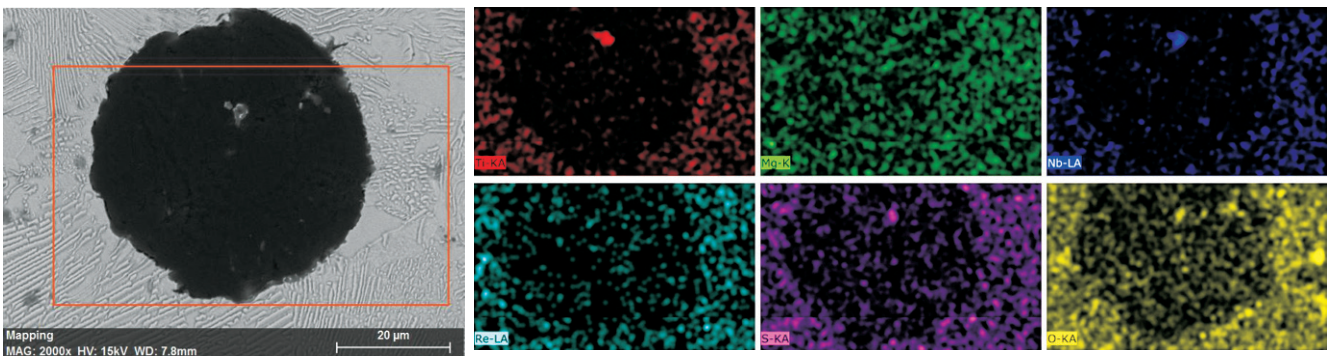
Fig. 3: Microstructure of as-cast QT700-6 alloy

Fig. 4: Energy spectrum of graphite core in as-cast QT700-6 alloy

addition was also prepared while other conditions remained the same. Figure 5 shows the tensile curves and graphite sizes of ductile cast iron with different niobium additions. Obviously, tensile properties of the alloy with 0.8% niobium (actual content of 0.75% niobium) are better than those of the alloy with 0.6% niobium, and the graphite size of the alloy with 0.8% niobium is significantly less than that of with 0.6% niobium. Increasing the content of niobium in a certain range is beneficial to improving the mechanical properties of ductile cast iron. However, the addition amount of niobium should be strictly controlled as niobium carbides will be formed around

the grain boundaries with too much niobium addition, and as a result, decrease the toughness of ductile iron cast.

Figure 6 shows the compositions and distribution of niobium carbides. A few carbide particles were found around the grain boundaries in as-cast QT700-6 alloy, as shown in Fig. 6(b). It is proved that these particles are niobium carbides according to the EDS analysis [Fig. 6(a)]. These 3–5 μm carbides without definite shape are mainly composed of iron, niobium and carbon elements, and they are beneficial to improving the strength of ductile iron [13]. However, when the content of niobium element is higher than 0.8%, a large amount of
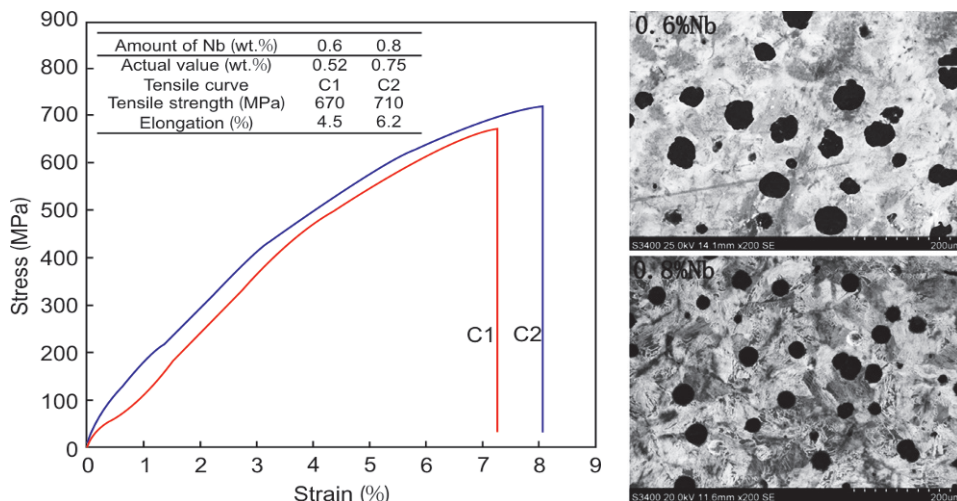

Fig. 5: Tensile curves and sizes of graphite with different amounts of niobium addition

El	Norm.C[wt.%]	Atom.C[at.%]
Nb	42.10	17.34
Fe	40.17	27.52
C	16.99	54.13

(a) Compositions of niobium carbides
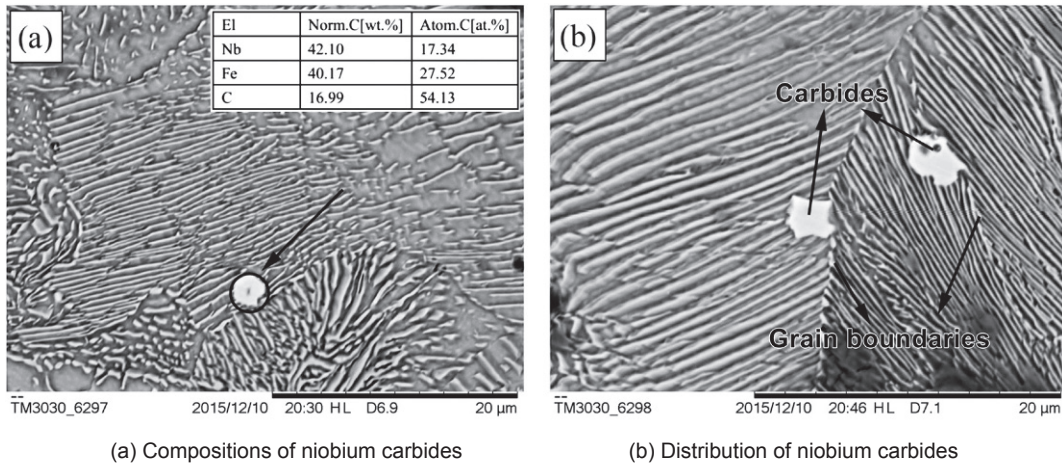
(b) Distribution of niobium carbides

Fig. 6: Element composition and distribution of niobium carbide

carbide particles will be detected around the grain boundaries in as-cast QT700-6 alloy, which deteriorate the toughness of ductile iron. In addition, niobium is very expensive, so there is no point to further increase the niobium content. Ductile iron cast with better comprehensive performance (the as-cast QT700-6 alloy) can be synthesized when the addition amount of niobium is 0.8%, and tensile strength and elongation of the as-cast QT700-6 alloy are over 700 MPa and 6%, respectively (Fig. 5a).

2.2 Refinement of lamellar pearlite in as-cast QT700-6 alloy

In general, pearlite lamellar spacing mainly depends on cooling rate, and the faster the cooling rate, the smaller the lamellar spacing [13]. Eutectoid transformation temperature of the alloy decreases with the addition of alloying elements, leading to an increase in undercooling (ΔT) and a decrease in pearlite lamellar spacing (S_0). According to the classic equation proposed by Marder [13]:

$$S_0 = C/\Delta T \qquad (3)$$

where C is a constant (= 8.02×10^3 nm·K), ΔT is undercooling, i.e. the difference between eutectoid transformation temperature and equilibrium critical transformation temperature of pearlite.

Figure 7(a) shows the morphology of local pearlite lamellar

in the as-cast QT700-6 alloy. It can be seen that the pearlite lamellar is composed of ferrite and cementite in alternate growth formation. It is clearly observed that the pearlite lamellar in this region forms in almost the same orientation. The pearlite lamellar spacing (L) can be approximately calculated as follows:

$$L = \pi d_c/Mn \qquad (4)$$

where d_c is the diameter of measuring circle, n is cut-off points of measuring circle and carbide, M is the magnification. The pearlite lamellar spacing of this area could be calculated by changing the diameter of measuring circle. Through adjusting the size of metallography to 150 mm × 112.5 mm in the drawing software, measuring circles with different diameters (10 mm, 15 mm, 20 mm, 25 mm, 30 mm and 35 mm) are marked in Fig. 7(a) to calculate the lamellar spacing. Figure 7(b) shows the relationship between diameter of measuring circle and lamellar spacing. Then, the average value is calculated from different measuring circles, and the local pearlite lamellar spacing is approximate 248 nm, indicating that the pearlite is in the form of sorbite.

Figure 8 shows the effect of alloying elements on pearlite lamellar spacing. Chemical compositions are confirmed using EDS in different regions as marked in Fig. 8. It is noticed that copper and nickel elements have a great effect on pearlite
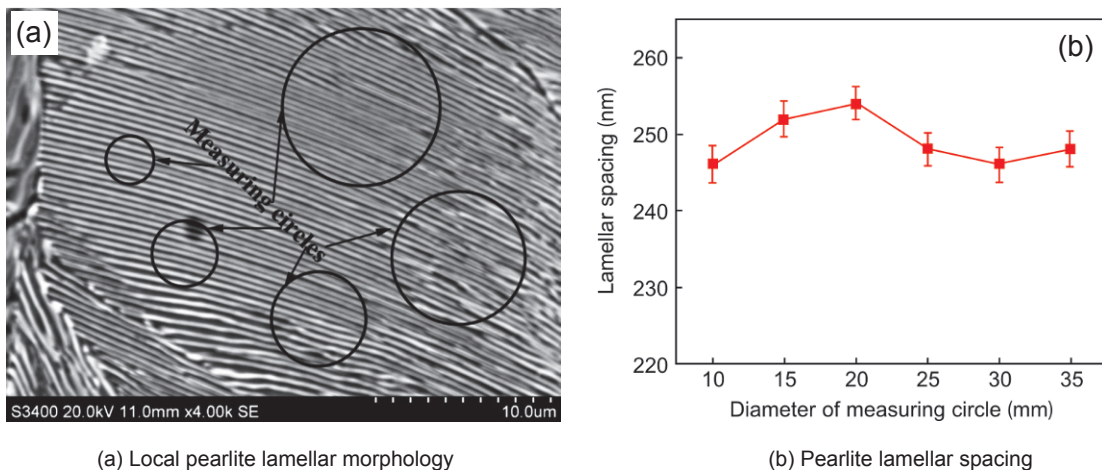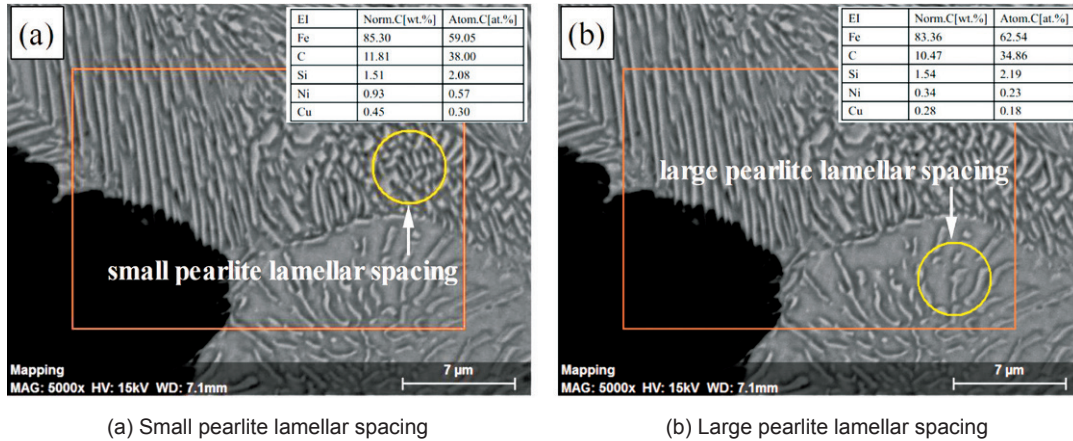

(a) Local pearlite lamellar morphology

(b) Pearlite lamellar spacing

Fig. 7: Morphology and spacing of local pearlite lamellar

(a) Small pearlite lamellar spacing

(b) Large pearlite lamellar spacing

Fig. 8: Effect of alloying elements on pearlite lamellar spacing

lamellar spacing. The content of nickel and copper is higher in the region marked in yellow circle in Fig. 8(a), the pearlite lamellar spacing of this region is smaller. While pearlite lamellar spacing of the neighboring region [yellow circle in Fig. 8(b)] is larger, and the content of nickel and copper is lower than that of the pearlite lamellar spacing in the Fig. 8(a). This is because the undercooling of the alloy may increase with the addition of alloying elements (Cu and Ni) [12], leading to the decrease of pearlite lamellar spacing, which is beneficial to improving the tensile strength of ductile cast iron.

2.3 Tensile fracture behavior of as-cast QT700-6 alloy

Figure 9(a) shows fracture morphology of the as-cast QT700-

6 alloy from the crack source to extended fracture. A small amount of dimples can be observed, which is conducive to the increase of elongation. Figure 9(b) shows river-pattern fracture and ladder morphology. The cracks' location is mainly at the interface between graphite and pearlite due to the low interfacial energy. Therefore, the graphite separates from the matrix under the effect of stress. With the increase of stress, cracks propagate to the other cracks formed by the neighboring graphite separating from the matrix. When the applied stress is over the fracture strength of pearlite, the fracture occurs. As can be seen from Fig. 9, almost no plastic deformation can be observed, indicating that the main fracture mechanism of as-cast QT700-6 alloy is cleavage fracture.
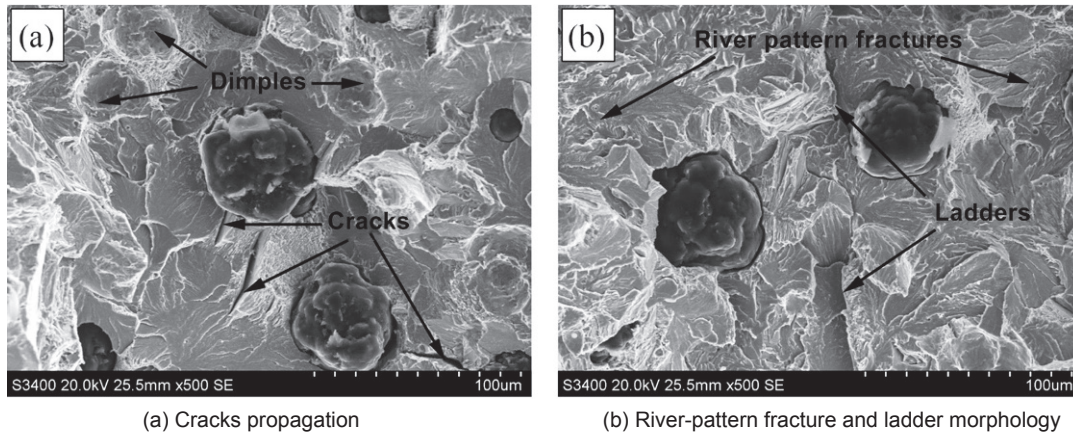
(a) Cracks propagation

(b) River-pattern fracture and ladder morphology

Fig. 9: Fracture morphology of as-cast QT700-6 alloy

Generally, fracture morphology displays continuous river-pattern morphology and the direction of crack propagation is along river-pattern shape in the ductile cast iron with pearlite matrix [22, 23]. In this work, when the pearlite matrix is subjected to the applied stress, plastic deformation mainly occurs at the ferrite regions and cementite layers, hindering the dislocation slip. For the pearlite lamellar in ductile cast iron, the maximum slip distance equals to lamellar spacing. Therefore, the smaller the lamellar spacing, the more the phase interfaces of the cementite and ferrite within a certain range, which is beneficial to the enhancement of the strength, i.e., plastic deformation

resistance will significantly increase, leading to an increase of strength and hardness of ductile iron.

3 Conclusions

(1) The as-cast QT700-6 alloy could be synthesized by alloying method, and the ratio of pearlite/ferrite is about 9:1 and the diameter of graphite is less than 40 μm.

(2) The predominant refinement mechanism of the graphite is attributed to the formation of niobium carbides, which acted as the heterogeneous nucleus, but they also exist around the grain

boundaries to improve the tensile strength in a certain range. The tensile strength and elongation of the as-cast QT700-6 alloy reach over 700 MPa and 6%, respectively, when the addition amount of niobium is 0.8%.

(3) The higher the content of nickel and copper, the smaller the pearlite lamellar spacing within a certain range in as-cast QT700-6 alloy. The local pearlite lamellar spacing is calculated as about 248 nm, indicating that the pearlite is in the form of sorbite.

(4) The main fracture mechanism of as-cast QT700-6 alloy is cleavage fracture with the appearance of a small amount of dimples.

References

[1] Di Cocco V, Iacoviello F, Rossi A, et al. Graphite nodules and fatigue crack propagation micromechanisms in a ferritic cast ductile iron. Fatigue & Fracture of Engineering Materials & Structures, 2013, 36(9): 893–902.

[2] Qi K, Yu F, Bai F, et al. Research on the hot deformation behavior and graphite morphology of spheroidal graphite cast iron at high strain rate. Materials & Design, 2009, 30(10): 4511–4515.

[3] Ji C, Zhu S. Study of a new type ductile iron for rolling: composition design (1). Materials Science and Engineering A, 2006, 419(1): 318–325.

[4] Martinez Celis M, Valle N, Lacaze J, et al. Microstructure of as cast reinforced ductile iron. International Journal of Cast Metals Research, 2011, 24(2): 76–82.

[5] Refaey A, Fatahalla N. Effect of microstructure on properties of ADI and low alloyed ductile iron. Journal of Materials Science, 2003, 38(2): 351–362.

[6] Murcia S C, Paniagua M A, Ossa E A. Development of as-cast dual matrix structure (DMS) ductile iron. Materials Science and Engineering A, 2013, 566(3): 8–15.

[7] Martins R, Seabra J, Magalhaes L. Austempered ductile iron (ADI) gears: Power loss, pitting and micropitting. Wear, 2008, 264(9): 838–849.

[8] Gonzaga R A. Influence of ferrite and pearlite content on mechanical properties of cast ductile irons. Materials Science and Engineering A, 2013, 567(4): 1–8.

[9] Putatunda S K. Development of austempered cast ductile iron (ADI) with simultaneous high yield strength and fracture toughness by a novel two-step austempering process. Materials Science and Engineering A, 2001, 315(1): 70–80.

[10] El-Baradie Z M, Ibrahim M M, El-Sisy I A, et al. Austempering of spheroidal graphite cast iron. Materials Science, 2004, 40(4): 523–528.

[11] Collini L, Pirondi A, Bianchi R, et al. Influence of casting defects on fatigue crack initiation and fatigue limit of cast ductile iron. Procedia Engineering, 2011, 10: 2898–2903.

[12] Cho G S, Choe K H, Lee K W, et al. Effects of alloying elements on the microstructures and mechanical properties of heavy section cast ductile iron. Journal of Materirals Science & Technology, 2007, 23(1): 97–101.

[13] Zhou W, Zhu H, Zheng D, et al. Niobium alloying effect in high carbon equivalent grey cast iron. Research & Development, 2011 8(1): 36–40.

[14] Romański, A, Tokarski, T, Tyrała, D. Sintered Fe-Ni-Cu-Sn-C alloys made of ball-milled powders. Archives of Metallurgy & Materials, 2014, 59(3): 947–950.

[15] Martínez R A. Fracture surfaces and the associated failure mechanisms in ductile iron with different matrices and load bearing. Engineering Fracture Mechanics, 2010, 77(14): 2749–2762.

[16] Nilsson K F, Blagoeva D, Moretto P. An experimental and numerical analysis to correlate variation in ductility to defects and microstructure in cast ductile iron components. Engineering Fracture Mechanics, 2006, 73(9): 1133–1157.

[17] Labrecque C, Gagne M. Ductile iron: fifty years of continuous development. Canadian Metallurgical Quarterly, 1998, 37(5): 343–378.

[18] Kocatepe K, Cerah M, Erdogan M. Effect of martensite volume fraction and its morphology on the tensile properties of ferritic ductile iron with dual matrix structures. Journal of Materials Processing Technology, 2006, 178(1): 44–51.

[19] Chaengkham P, Srichandr P. Continuously cast ductile iron: processing, structures, and properties. Journal of Materials Processing Technology, 2011, 211(8): 1372–1378.

[20] Aksoy M, Kuzucu V, Korkut M H. The influence of strong carbide-forming elements and homogenization on the wear resistance of ferritic stainless steel. Wear, 1997, 211(2): 265–270.

[21] Filipovic M, Kamberovic Z, Korac M, et al. Wear resistance and dynamic fracture toughness of hypoeutectic high-chromium white cast iron alloyed with niobium and vanadium. Materiali in Tehnologije, 2014, 48(3): 343–348.

[22] Hebel J, Dieringer R, Becker W. Modelling brittle crack formation at geometrical and material discontinuities using a finite fracture mechanics approach. Engineering Fracture Mechanics, 2010, 77(18): 3558–3572.

[23] Cavallini M, Di Bartolomeo O, Iacoviello F. Fatigue crack propagation damaging micromechanisms in cast ductile irons. Engineering Fracture Mechanics, 2008, 75(3): 694–704.